NOTICE CONCERNING COPYRIGHT RESTRICTIONS

Resistivity Structure of the Silali Geothermal Prospect in Kenya

Deflorah Kangogo

Geothermal Development Company Ltd, Nakuru, Kenya
dkangogo@gdc.co.ke

Keywords

Geothermal, Kenyan north rift, resistivity structure, magnetotellurics, transient electromagnetic, steam dominated reservoir, heat source

ABSTRACT

Geophysical surveys comprising of Magnetotelluric (MT) and Transient Electromagnetic (TEM) methods were carried out in Silali geothermal prospect in the Kenyan north rift in order to image the resistivity distribution within the earth to depths of many kilometers which is then interpreted in terms of lithology.

Joint 1-D Inversion results of Transient Electromagneti>c (TEM) and Magnetotelluric (MT) data reveals a resistivity structure consisting of a shallow high-resistivity zone (> 100 Ωm), in about the uppermost 600m, underlain by low resistivity zone (10 Ωm)) to depths of about 1 kilometre and a deeper high resistivity (>50 Ωm) up to 3-4 km from the surface which is probably the steam dominated reservoir, again underlain by lower resistivity (about 4 km) which is interpreted as the heat source.

1.0 Introduction

Initial regional exploration for geothermal resources in Kenya indicated that the Quaternary volcanic complexes of the Kenya rift valley provided the most promising prospects for geothermal exploration. Consequently, detailed exploration for geothermal power has been concentrated around volcanic centres within the rift valley. Studies show that these centres have positive indications of geothermal resource that can be commercially developed. The geothermal potential of the area is associated with the magma chambers as the heat sources. Magnetotelluric (MT), seismic and magnetic data show that the heat sources are directly beneath the volcanic centres. This paper concentrates on the geophysical work that has been carried out in the Silali Geothermal prospect (Figure 1).

The Magnetotelluric (MT) technique, a natural electromagnetic method, has proved effective in mapping the characteristics of geothermal fields due to its lateral resolution and also greater depth of investigation. Magnetotellurics surveys are more appropriate for difficult topography due to their simple logistics and low cost compared to seismic surveys. MT provides useful information about the lateral and vertical resistivity variations in the earth's subsurface from surface measurement of two horizontal electric field and three magnetic field variations over a typical 10^{-3}-10^{3}

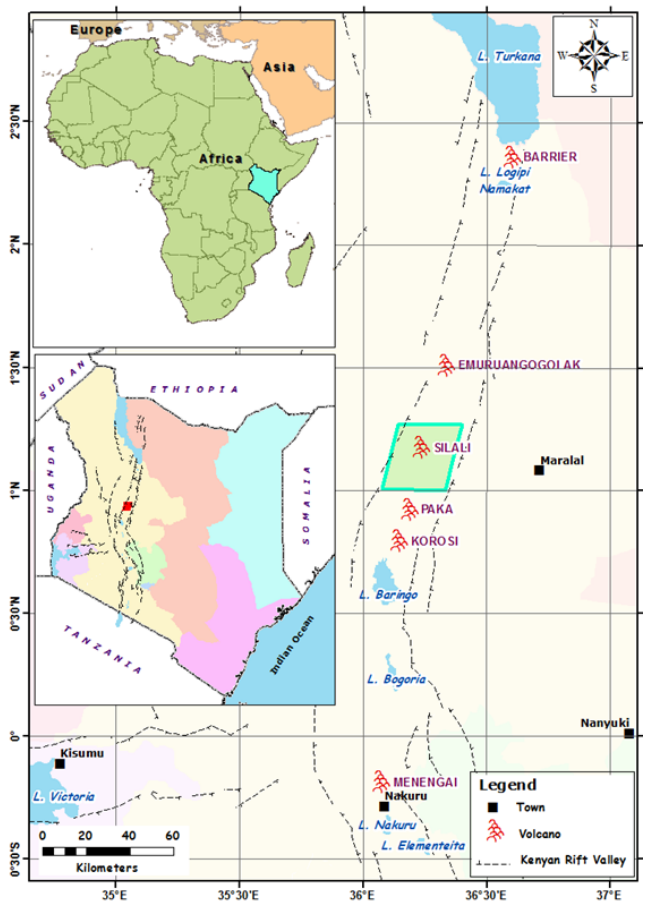

Figure 1. Map of Kenya rift showing Silali and other Kenya Northern rift sector volcanoes.

Hz frequency range. MT results along a profile can be used to evaluate the resource potential of the area. Data collected using magnetotellurics is used to determine the resistivity distribution within the earth to depths of many kilometers which is then interpreted in terms of lithology. The contrast in resistivities provides an excellent tool for identifying geothermal targets.

1.1 The Role of Electrical Resistivity

Apart from direct surface manifestations, the resistivity of subsurface rocks is the most diagnostic parameter of geothermal activity that can be measured from the surface. Rocks containing geothermal fluids have different resistivities than cold rocks. Most commonly the geothermal water lowers the resistivity, but in some cases the resistivity increases again at very high temperatures.

There are mainly two reasons why the geothermal activity lowers the resistivity. Firstly, the geothermal fluid has higher concentration of dissolved ions (higher salinity) than cold groundwater and is therefore more conductive. Secondly the thermal water interacts with the host rocks, forming secondary alteration minerals. Some of these minerals, such as clay minerals (smectite and zeolites), are conductive and reduce the resistivity of the rock formation. The type of alteration minerals that are formed depends on the host rock, the salinity of the fluid and temperature. At relatively low temperatures (lower than 180-200°C) the alteration minerals are commonly conductive, but at higher temperatures (higher than 200-240°C) the minerals are dominantly resistive. The temperature where the transition from conductive to resistive minerals occurs depends on the rock type. In acidic rocks it occurs at about 180-200°C, but in basic rocks it happens at about 220-240°C (Árnason et.al, 2000).

In a typical high-temperature geothermal systems (high-temperature systems have temperatures higher than 200°C above 1 km depth) in porous and permeable rocks, often have widespread resistivity anomalies characterised by a low resistivity cap at the outer margins which is underlain by higher resistivity in the core of the system, (Figure 2).

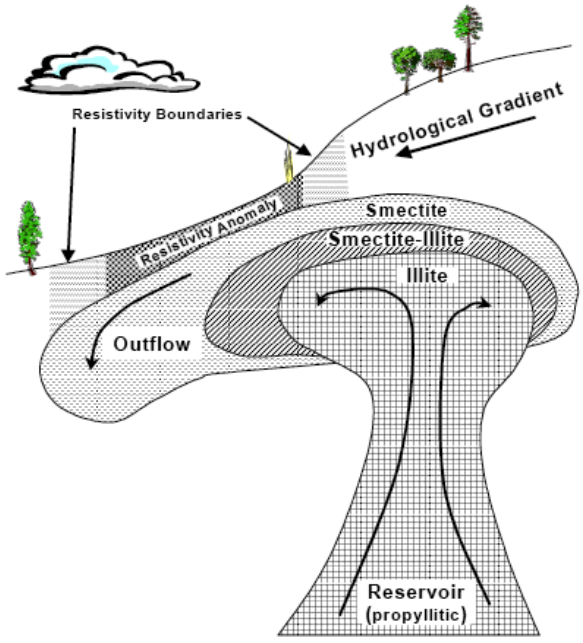

Figure 2. A typical High temperature geothermal system.

2.0 Methodology

2.1 MT Sounding

MT techniques measure over a frequency range. The lower the frequency, the greater the depth of investigation possible at a given site. MT techniques acquire data in frequencies ranging from about 400-0.0000129 Hz (over a period of about 21.5hrs), and are suitable for deeper investigations. The survey was planned so that work crews could set up one or more sites each day (depending on the nature of the terrain), allowing the equipment to acquire data for a period of time and then retrieving the equipment to re-deploy it at another site. In this survey, the equipment was left to acquire data overnight and retrieval usually happened the next morning.

Although an MT can be used alone, the best results are achieved when a remote or far remote site is available for noise-reduction techniques. Apart from the 50 Hz or 60 Hz grid frequency, electrical noise from human activities tends to vary considerably over distance. The natural magnetic signal, though, tends to be the same over large distances; the lower the frequency, the less variation. The MT equipment system employed took advantage of these characteristics by collecting data simultaneously at the survey ("local") sites and at one reference ("remote") site.

MT equipment and sensors must be calibrated before acquiring data. Calibration took place at the beginning of the survey, and was repeated in the course of the survey when equipment problems arose (e.g., damaged cables). The field layout comprised of two orthogonal electric dipoles to measure the two horizontal components, and two magnetic sensors parallel to the electric dipoles to measure the corresponding magnetic components. A third sensor measured the vertical magnetic component. Thus, at each station, five parameters were measured simultaneously as a function of frequency. By measuring the changes in the magnetic field (H) and electric (E) field over range frequencies, an apparent resistivity sounding curve can be produced, analogous to that produced for electrical resistivity sounding but measured as a function of frequency rather than inter-electrode separation. The data are displayed on log-log plots as apparent resistivity versus either frequency (f) or period ($1/2\pi f$)

3.0 Data Processing and Analysis

3.1 Resistivity

Both MT and TEM data can be analysed in different ways according to the manner in which they have been acquired. Measured parameters may be plotted as profiles or as gridded and contoured maps on which anomalous zones can be identified. These approaches tend to be qualitative and of first order interpretations. The data was processed, inverted and produced in apparent resistivity plots in form of contours maps at various elevations. The aim was to locate a possible sub-surface resistivity anomaly on the basis of relevant parameters such as apparent resistivity values, shape and size.

Time series processing included visual inspection of the recorded data and excluding disturbances and heavily noise affected parts of the time series. Although very time consuming this approach proved to be the best means to extract maximum information from the noise contaminated time series. These preconditioned time series were then transformed into the frequency

domain by a Fast Fourier Transform (FFT) using adapted window lengths. With a coherency based algorithm the Fourier spectra were then averaged and the impedance tensor estimated. The impedance tensor has been rotated mathematically by a constant angle derived from the swift angle at low frequencies. This results in a data set with consistent orientation with one axis approximately along the valley which is taken as direction for the E-field. Static shifts of the resistivity curves have been removed by means of the MT response derived from transent electromagnetotelluric (TEM) measurements at the same locations. Figure 3 and 4 below shows the map of the areal distribution of the resistivity soundings from the greater Silali prospect area.

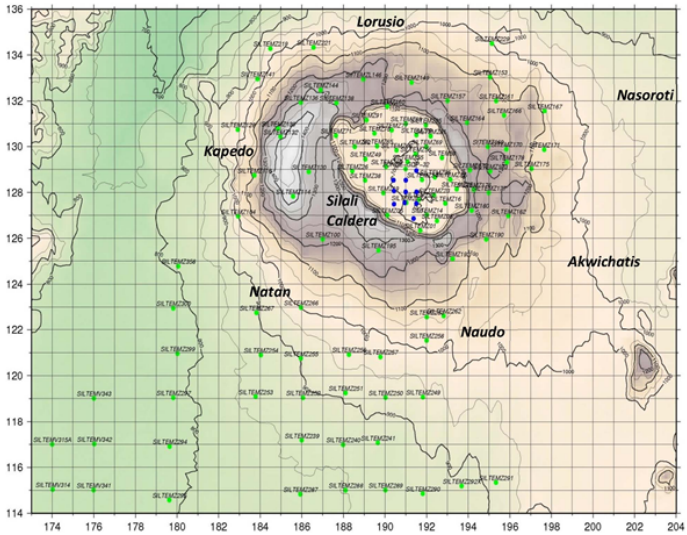

Figure 3. Map showing TEM locations stations in Silali geothermal prospect.

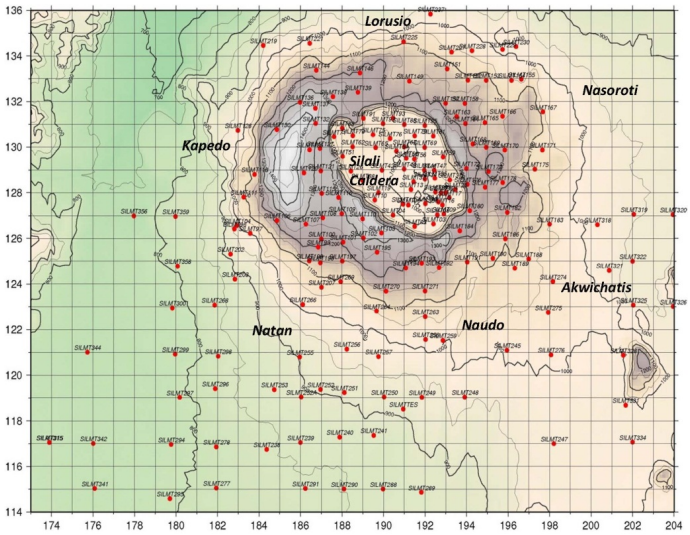

Figure 4. The areal distribution of MT resistivity soundings from the Silali prospect area.

Since resistivity of the subsurface varies with depth as well as horizontally, several iso-resistivity maps were constructed at elevations from 600 masl to 8000 mbsl as shown in Figures 5,6,7,8,9, and 10 respectively. The entire map indicates the prospect area.

b) Resistivity at 600 m.asl

This elevation is about 500-600 m below the surface (Figure 5). The map shows a low resistivity anomally of about 3.2 ohm-m in the caldera and on the eastern and western sides of the prospect area. This conductivity as seen above could be related to the hydrothermal products present at this depth. Also seen in the map is a high resistivity anomally of about 56 ohm-m on the Southern side of the survey area trending in the NE-SW direction due to unaltered formations and its along the major fault line cutting through the caldera in the western portion of the region.

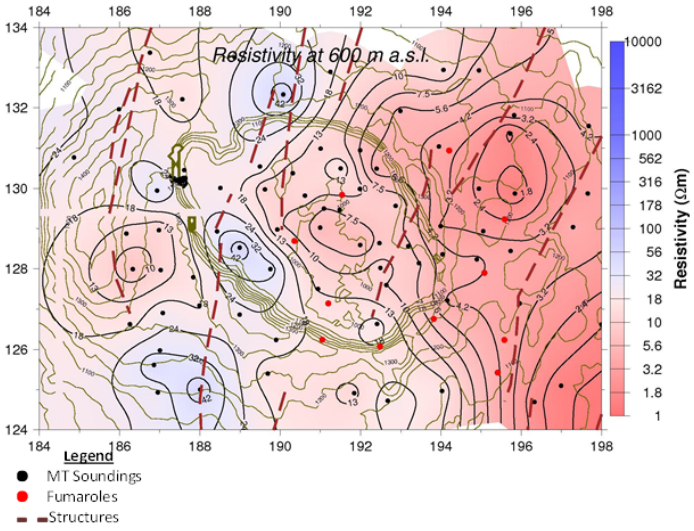

Figure 5. Resistivity anomaly map at 600 m above sea level (masl).

(d) Resistivity at Sea Level

The map shows relatively high resistivity anomalies of about 56 ohm-m in the central portion of the map and trending in the NW-SE directions, and seems to be extending to the east out of the caldera (Figure 6). This higher resistivity is probably defining the steam dominated reservoir for this sector of the prospect . Low resistivities of aboue 5.6 ohm-m are also evident in the southwest and northeast of the map bounding the high resistivity zone. These

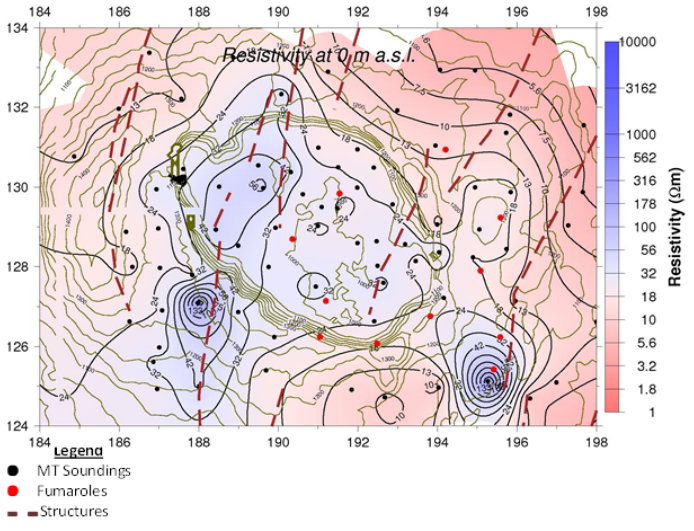

Figure 6. Resistivity anomaly map at sea level.

low resistivities are defining areas where low temperature alteration is still present from 800m above sea level

(e) Resistivity at 400 m. bsl

At 400 m below sea level (Figure 7), a high resistivity of about 56 ohm-m is still evident and seems to extend out of the caldera in the NW. This still defines the extent of the steam dominated reservoir at that elevation. Elsewhere demarcating the high resistivity is a lower resistivity all-round the prospect due to hydrothermal alteration.

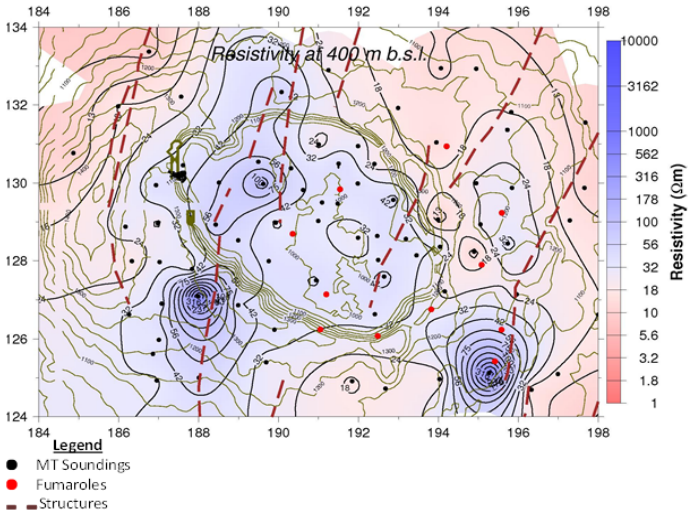

Figure 7. Resistivity anomaly map at 400 m below sea level.

(f) Resistivity at 1000 m. bsl

Similarly at this level the high resistivity persists which indicates that the high temperature alteration mineral are at play (Figure 8). Elsewhere a low resistivity appears to the east of the caldera aligning in the N-S direction. This could be a fluid dominated fracture zone.

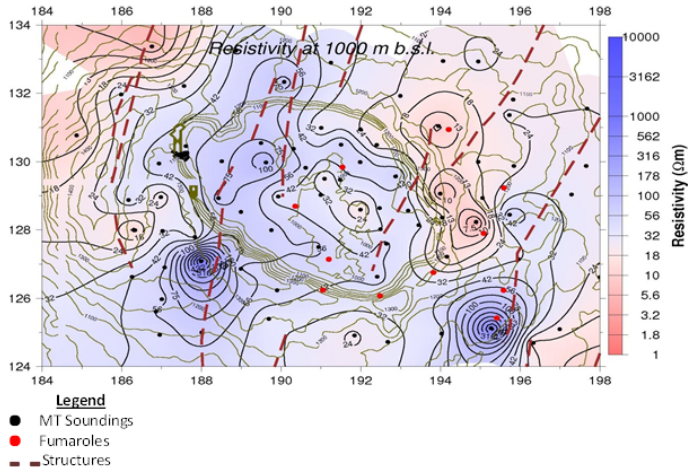

Figure 8. Resistivity anomaly map at 1000 m below sea level.

(f) Resistivity at 3000 mbsl

At 3000 m below sea level (Figure 9), the deeper conductors are evident from the eastern part of the prospect area and extending towards the central part of the caldera. These conductors could be defining the top of the heat sources for this sector. A linear high resistivity is also evident aligning along the western rim of the caldera which could be a boundary (structure) separating the resource inside the caldera and the one towards Kapedo.

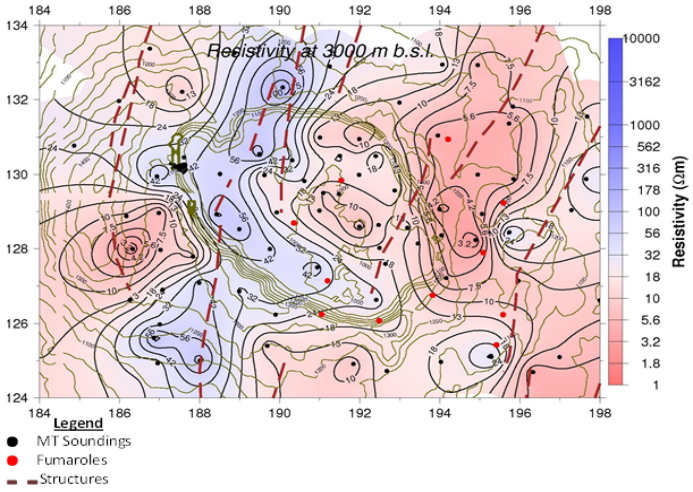

Figure 9. Resistivity anomaly map at 3000 m below sea level.

The deep conductor seems to be extending towards the eastern part of the prospect where a number of surface manifestations are evident including fumaroles and hot grounds.

(g) Resistivity at 5000 m. bsl

A low resistivity anomaly spreads almost in the entire survey area with more prominence in the eastern part of the prospect area from the centre of the caldera (Figure 10). This probably is a heat source extending towards the Eastern part of the prospect area. The relatively high resistivity seen in the upper elevation is still present which shows that the heat source is structurally controlled.

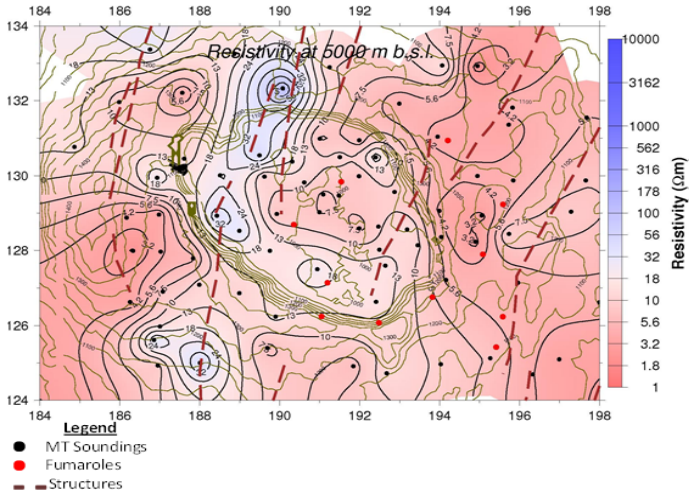

Figure 10. Resistivity anomaly map at 5000 m below sea level.

3.4.3 Cross-Sections

Two of the sections are in SW-NE and two others in NW-SE for both MT and TEM (Figure 12). These sections have been done using 1D inversion. The smoothed Occam's models have

consistently defined resistivity values (from the inversion) at different depths and an automatic contouring and colouring of the resistivity was applied. TEM cross-section was chosen to resolve resistivities at shallow depths and MT to resolve resistivities at deeper levels since it has a poor resolution at shallow depths due to static shift that the MT suffers.

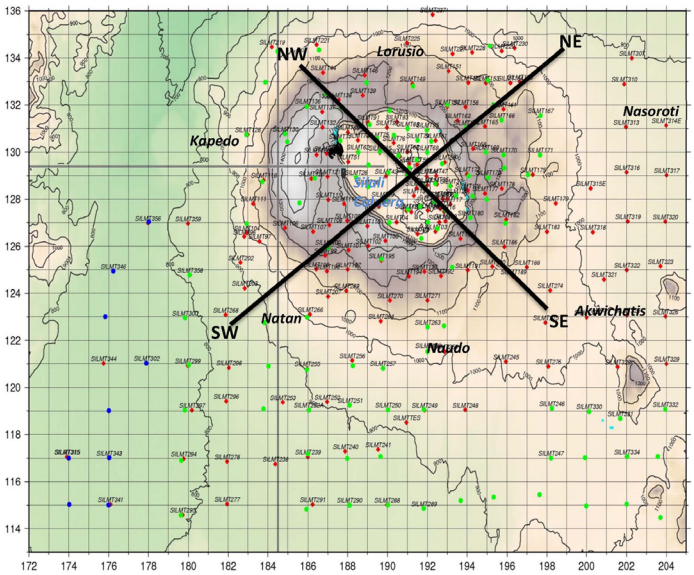

Figure 11. Cross section map showing profiles across the Prospect area.

(a) MT Cross-section NW-SE

In the central portion below the Silali prospect a high resistivity anomaly is evident which represents the major structure on the western part of the prospect at depth (Figure 13). A low resistivity anomally is evident at about 2 km depth and which seems to be extending towards the eastern side of the caldera and which is interpreted as the heat source for this geothermal system. It is overlayed by a high resistivity anomaly at around 1km below sea level and extending eastwards and this represents the reservoir level for this geothermal system.

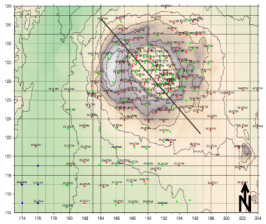

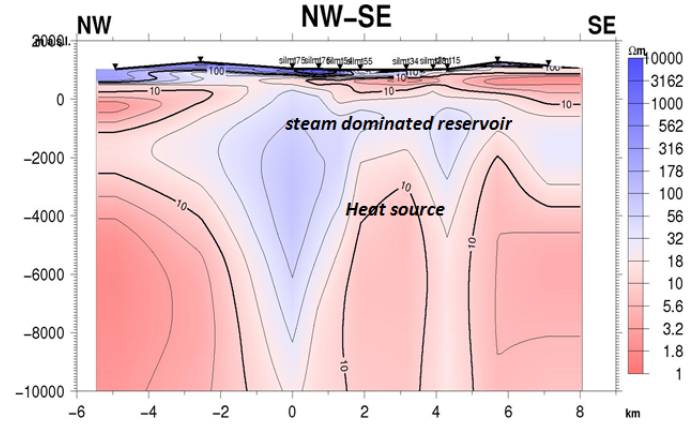

Figure 12. 2D Resistivity cross-section along NW-SE.

(c) MT Cross-Section SW-NE

The section (Figure 14) shows two distinct low resistivity anomalies from a depth of 3 km. One is in the central part of the caldera and the other is extending towards the eastern side of the caldera. These deeper conductors are imaging the heat sources for this prospect. The anomaly extends further East outside the caldera towards Akwichatis and Nasoroti areas which is the heat source for this geothermal system.

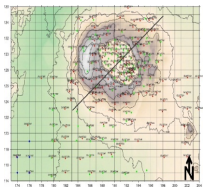

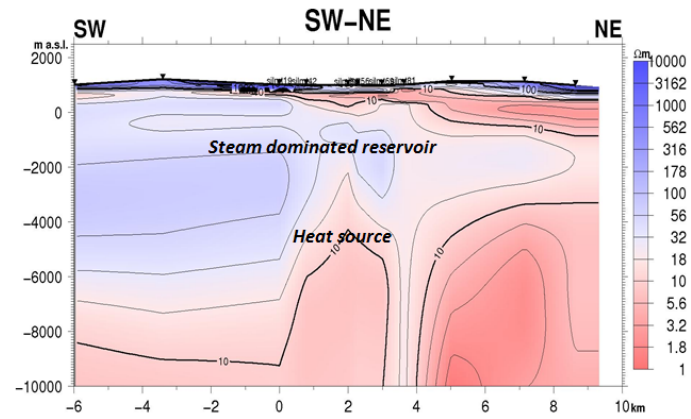

Figure 13. 2-D Resistivity cross-section along SW-NE.

4.0 Discussions

This resistivity survey reveals a resistivity structure consisting of a shallow high-resistivity layer, in about the uppermost 600m, underlain by low resistivity. At greater depth, a second high-

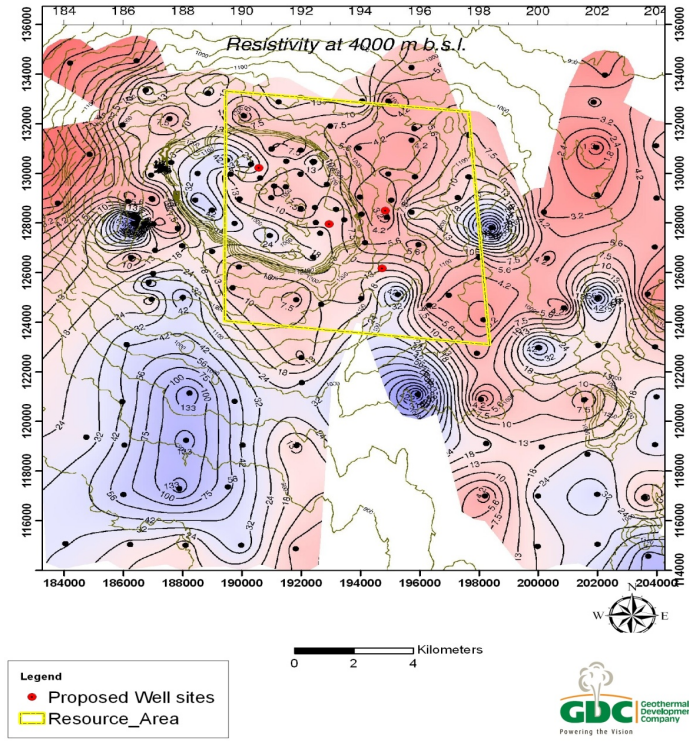

Figure 14. Silali proposed exploratory well sites and resource area.

resistivity layer is observed in most of the area at about 2km from the surface which is probably the steam dominated reservoir, again underlain by lower resistivity (about 4 km) which is interpreted as the heat source.

5.0 Conclusion

The resource area based on the anomaly is about 60 km^2 which can yield about 900 MWe based on the world average of 15 MWe/km^2

6.0 References

Cumming, W., Mackie, R., (2010). Resistivity imaging of geothermal resource using 1D, 2D, and 3D MT inversion and TDEM static shift correction illustrated by a Glass mountain case history. Proceeding World Geothermal Congress, 2010.

Flovenz, O., Spangenberg, E., Kulenkampff, J., Anarson, K., Karlsdottir, R., and Huenge, E. (2005). The role of electrical conduction in geothermal exploration. Paper presented at the World Geothermal Congress, Antalya, Turkey.

Lichoro, 2009., Joint 1-D inversion of TEM and MT data from Olkaria domes geothermal area, Kenya. Paper presented at the UNU geothermal Training Programme.

Newman, G. A., Hoversten, M.,Gasperikova, E., Wannamaker, P. E., (2008). Three-dimensional magnetotelluric characterization of the Coso geothermal field Geothermics 37, 369-399

Pellerin, L., Johnston, J. M., Hohmann, G. W., (1996). A numerical evaluation of electromagnetic methods in geothermal exploration. Geophysics. 61, 121-130.

Wright, P. M., Ward, S. H., Ross, H. P., West, R. C., (1985). State-of-the-art geophysical exploration for geothermal resources. Geophysics, 55. 2666-2699.